Molecular Genetics and Metabolism xxx (xxxx) xxx

Contents lists available at ScienceDirect

Molecular Genetics and Metabolism

journal homepage: www.elsevier.com/locate/ymgme

Compound heterozygosis in AADC deficiency: A complex phenotype dissected through comparison among heterodimeric and homodimeric AADC proteins

Carmen Longo [a,1], Riccardo Montioli [a,1], Giovanni Bisello [a,1], Luana Palazzi [b], Mario Mastrangelo [c], Heiko Brennenstuhl [d], Patrizia Polverino de Laureto [b], Thomas Opladen [d], Vincenzo Leuzzi [c], Mariarita Bertoldi [a,*]

[a] Department of Neuroscience, Biomedicine and Movement Sciences, Section of Biological Chemistry, Strada Le Grazie 8, 37134 Verona, Italy
[b] Department of Pharmaceutical and Pharmacological Sciences, CRIBI Biotechnology Center, University of Padua, Padua, Italy
[c] Unit of Child Neurology and Psychiatry Unit, Department of Human Neuroscience, Sapienza University of Rome, Italy
[d] University Children's Hospital Heidelberg, Department of General Pediatrics, Division of Neuropediatrics and Metabolic Medicine, Heidelberg, Germany

ARTICLE INFO

Article history:
Received 30 April 2021
Received in revised form 25 August 2021
Accepted 25 August 2021
Available online xxxx

Keywords:
Aromatic amino acid decarboxylase
AADC deficiency
Pyridoxal 5′-phosphate
Enzymatic variants

ABSTRACT

Compound heterozygosis is the most diffuse and hardly to tackle condition in aromatic amino acid decarboxylase (AADC) deficiency, a genetic disease leading to severe neurological impairment. Here, by using an appropriate vector, we succeeded in obtaining high yields of AADC protein and characterizing two new heterodimers, T69M/S147R and C281W/M362T, detected in two AADC deficiency patients. We performed an extensive biochemical characterization of the heterodimeric recombinant proteins and of the related homodimers, by a combination of dichroic and fluorescence spectroscopy and activity assays together with bioinformatic analyses. We found that T69M/S147R exhibits negative complementation in terms of activity but it is more stable than the average of the homodimeric counterparts. The heterodimer C281W/M362T retains a nearly good catalytic efficiency, whereas M362T homodimer is less affected and C281W homodimer is recovered as insoluble. These results, which are consistent with the related phenotypes, and the data emerging from previous studies, suggest that the severity of AADC deficiency is not directly explained by positive or negative complementation phenomena, but rather depends on: i) the integrity of one or both active sites; ii) the structural and functional properties of the entire pool of AADC proteins expressed. Overall, this integrated and cross-sectional approach enables proper characterization and depicts the functional result of subunit interactions in the dimeric structure and will help to elucidate the physio-pathological mechanisms in AADC deficiency.

1. Introduction

Aromatic amino acid decarboxylase (AADC) deficiency is a severe autosomal recessive monogenic disorder (OMIM #608643) caused by mutations in the *DDC* gene located on chromosome 7 band p12.1-p12.3 [1], (GRCh38.p13; chr7: 50,447,733-50,576,163). The subsequent AADC misfunctioning or loss-of-function results in an impaired conversion of L-Dopa or L-5-hydroxytryptophan into their amine products, dopamine and serotonin.

Clinical presentation of patients with AADC deficiency include movement disorders (such as oculogyric crisis, hypokinesia, muscular hypotonia or hypertonia, and dystonia), neurodevelopmental delay, sleep and mood disturbances, orthostatic hypotension, chronic diarrhea, hypoglycemia [1,2]. The wide range of clinical presentation and outcome severity is ascribed to the characteristics of the genetic alteration (missense, frame-shift, deletions) which would result in protein variants with different residual enzymatic activity. Comprehensive studies aimed to correlate the type of amino acid alteration to the lost or changed protein function have been previously published [3–7].

A recent review on AADC deficiency [1] underlines that, among known genotypes, 67% are compound heterozygous and adding the most updated data of 2020, this percentage rises up to 71%. This means that the number of newly identified heterozygous patients is growing, differently from the situation in 2014 [3] when the identified patients were mostly homozygous.

Abbreviations: AADC, aromatic amino acid decarboxylase; PLP, pyridoxal 5′-phosphate; CD, circular dichroism; WT, wild-type.

* Corresponding author.
E-mail address: mita.bertoldi@univr.it (M. Bertoldi).

[1] These authors contributed equally.

https://doi.org/10.1016/j.ymgme.2021.08.011
1096-7192/

Given this complex situation, past investigations tried to unravel the molecular basis of the phenotype of heterozygous patients by producing recombinant heterodimeric AADC and a positive [6] and negative [7] interallelic complementation has been claimed, respectively. However, an extremely low yield in heterodimeric species, possibly due to the type of variant or to the expression system based on co-expression of two vectors, affected those studies and could have prevented a complete characterization.

AADC deficiency is one of a few genetic diseases for which interallelic complementation has been studied. In phenylketonuria, phenylalanine hydroxylase shows negative and positive complementation [8]. For arginine succinate lyase, interallelic complementation explains the heterogeneity found in the related genetic disease [9]. In methylmalonyl-CoA mutase deficiency [10,11] and primary hyperoxaluria type I [12], a positive interallelic complementation was demonstrated for few variants deriving from different alleles.

Here, by using an optimized method to produce heterodimeric AADC proteins in larger amounts, we lay the groundwork to characterize the structural and functional features of two heterodimers T69M/S147R and C281W/M362T, together with the associated homodimer counterparts, and compare them to the clinical phenotype of related AADC compound heterozygous patients. We demonstrate that a combined approach of *in vitro* and *in silico* analyses can ultimately improve our understanding of rare monogenic diseases and help to find a better genotype-phenotype correlation mechanism.

2. Materials and methods

2.1. Materials

Pyridoxal 5′-phosphate (PLP), L-Dopa, dopa methylester (DME), hydroxylamine hydrochloride, isopropyl-β-d-thiogalactopyranoside (IPTG), trinitrobenzenesulfonic acid (TNB), phenylmethylsulfonyl fluoride (PMSF), trichloroacetic acid (TCA) and Sigmafast™ protease inhibitor cocktail (P8849) were purchased from Sigma. Anti AADC monoclonal antibody (8E8) and mouse IgG kappa binding protein (m-IgGk BP) conjugated with horseradish peroxidase (HRP) were purchased from Santa Cruz Biotechnology, anti-Strep mAb from Abcam and anti-His mAb from Genscript. All other chemicals were of the highest purity available.

2.2. His/StrepAADC vector construction and site-directed mutagenesis

To construct the expression vector for the heterodimeric AADC, pETDuet-1 (Merck) was chosen. Two multiple cloning sites are available in this plasmid, each one under the control of an independent T7 promoter: in the first site the cDNA for AADC endowed with 6xHis tag at the C-terminus [3] was subcloned exploiting *Nco*I and *Hin*dIII as restriction sites, whereas in the other one the cDNA for AADC endowed with a C-terminal Strep-tag-II [13] was subcloned exploiting *Nde*I and *Xho*I (ThermoFisher). Firstly, StrepAADC cDNA was subcloned in pETDuet-1, and this plasmid was then used for StrepAADC expression. Secondly, the cDNA for HisAADC was subcloned in the same pETDuet-1-StrepAADC plasmid, thus leading to the final construct pETDuet-1-His/Strep AADC, a vector expressing both HisAADC and StrepAADC in 1:1 ratio. In order to obtain the cDNAs of the HisT69M, StrepS147R, HisC281W and StrepM362T proteins, the variants T69M, S147R, C281W and M362T were introduced in the pETDuet-1-HisAADC or pETDuet-1-StrepAADC expression vector by site directed mutagenesis using Quik-Change II site directed mutagenesis kit (Agilent Technologies) with the primers listed in Table 1S. All mutations were confirmed by DNA sequence analysis of the whole open reading frame. The mutant cDNAs were then subcloned from the pETDuet-1-HisS147RAADC or pETDuet-1-HisC281WAADC or pETDuet-1-HisM362TAADC to the pETDuet-1-StrepT69MAADC or pETDuet-1-StrepM362TMAADC or pETDuet-1-StrepC281WMAADC, respectively to construct the T69M/S147R and C281W/M362T heterodimer expression plasmids following the same cloning strategy adopted to prepare the wild-type pETDuet-1-His/StrepAADC.

2.3. Expression and purification of AADC variants

The obtained construct was used to transform chemically competent BL21(DE3) *E. coli* by heat shock at 42 °C. One colony was brought into 150 mL of Luria Bertani (LB)-broth supplemented with ampicillin (Amp) (100 mg/L Amp) and scaled up to 4.5 L of LB-broth/Amp. Bacteria were grown at 37 °C until optical density (OD) at 600 nm was 0.5–0.6. Expression was induced with 0.1 mM IPTG for 18 h at 30 °C. One hour before induction PLP was added to the cell culture in different concentrations, depending on the AADC variant: 20 μM for the wild-type (WT) AADC, 50 μM for T69M and M362T and 100 μM for S147R, C281W, T69M/S147R and C281W/M362T AADC variants. Bacteria were harvested at 5500 rpm, 4 °C, 10′ and pellets were resuspended in different buffers depending on the tag carried by the expressed protein: 20 mM sodium phosphate buffer pH 7.4, 0.5 mM sodium chloride, 20 mM imidazole was used for His-tagged homodimeric variants and for His-Strep heterodimeric ones, whereas Strep-tactin buffer (20 mM sodium phosphate pH 7.4, 280 mM sodium chloride and 6 mM potassium chloride) was used for Strep-tagged proteins. Both of the resuspension buffers were also supplemented with 50 μM PLP, 0.5 mM PMSF and protease inhibitor cocktail. Cell lysis was achieved by adding 0.2 mg/mL lysozyme for 20′ at room temperature. After shock-freeze in liquid nitrogen, bacterial lysates were stored at −80 °C or carefully thawed at room temperature, filtered on gauze and loaded either on a HisPrep FF 16/10 (GE Healthcare) (wild-type His/Strep AADC, HisT69M/StrepS147R, HisT69M and HisM362T AADC variants) or on a HisTrap FF crude column (GE Healthcare) (HisC281W/StrepM362T AADC variant) and eluted applying a linear gradient of imidazole (20 mM to 500 mM in 10 column volumes, flow 1 mL/min). Strep-tagged AADC bacterial lysates were loaded on a StrepTrap column (GE Healthcare) and eluted with 2.5 mM desthiobiotin dissolved in Strep-tactin buffer.

For the purification of heterodimeric His/Strep AADC variants, the two purification steps were applied consequentially, thus resulting in the purified heterodimeric species. In fact, when loading the cell lysate on a HisTrap column the Strep-tagged homodimeric AADC is eliminated in the flowthrough, since it has no affinity for the resin. Conversely, loading the eluted fraction from step 1 on the StrepTrap column leads to the elimination of the homodimeric His/His AADC in the flowthrough and the final elution of the heterodimeric His/Strep AADC at a high purity (Fig. 1S). In between the two steps, the eluted fraction from HisPrep column was washed with Strep-tactin buffer using Amicon Ultra 10 kDa MWCO concentrators (Millipore). After step 2, the eluted fraction was likewise washed with 100 mM potassium phosphate buffer pH 7.4 and the protein concentration was determined by using a ε_M of 142,000 M^{-1} cm^{-1} (homodimeric His AADC), 150,000 M^{-1} cm^{-1} (homodimeric Strep AADC) and 146,000 M^{-1} cm^{-1} (heterodimeric His/Strep AADC). PLP content of the purified AADC variants was determined by releasing the coenzyme in 0.1 M NaOH and by using a ε_M of 6600 M^{-1} cm^{-1} at 388 nm [5].

The purity of the heterodimeric His/Strep AADC was assessed by SDS-PAGE and the presence of the two different tags was controlled by performing three Western Blot analyses, incubating with different primary monoclonal antibodies, anti-AADC, anti-His and anti-Strep, as reported under Materials. Each membrane was then incubated with the secondary antibody (see Materials) and the signal was detected using Immobilon Western Chemiluminescent HRP Substrate (Merck-Millipore) and a ChemiDOC XRS+ Imaging System (Bio-Rad).

2.4. Size-exclusion liquid chromatography

Size-exclusion liquid chromatography was applied an additional orthogonal purification step. Samples were loaded on a Superdex 200 (10/

300) (GE Healthcare) column equilibrated with 100 mM potassium phosphate buffer pH 7.4, on an Akta FPLC system (GE Healthcare). The run was performed using the same buffer at a flow rate of 0.3 mL/min with detection at 280 nm.

2.5. Apoenzyme preparation and coenzyme binding affinity measurements

Apoenzyme was obtained by incubating 5 μM holoenzyme with 10 mM hydroxylamine in 0.5 M potassium phosphate buffer pH 6.8 at 25 °C for 3 h as reported [5]. The equilibrium apparent dissociation constant for PLP, $K_{D(PLP)}$, was determined as reported [5]. Curve fitting was performed using Origin® 9.1 Pro (OriginLab).

2.6. Enzyme activity assays

Decarboxylase activity was measured by a stopped spectrophotometric assay [14,15]. Each enzymatic variant (at 0.15 μM, unless otherwise stated) was incubated under saturating PLP concentration (10 μM) and different L-Dopa concentrations (from 0.05 to 2 mM) in a final volume of 250 μL in 100 mM potassium phosphate buffer pH 7.4 for a time period in which a linear product formation is observed and quantitated as reported [4]. The kinetic parameters were determined by fitting the data obtained with the Michaelis-Menten equation using Origin® 9.1 Pro (OriginLab).

2.7. HPLC analysis of coenzyme modification and dopamine formation

The enzymatic assay for T69M/S147R AADC variant was performed at 1.5 μM concentration, 25 μM PLP at increasing L-Dopa concentrations (from 0.2 to 8 mM) in a final volume of 225 μL. The reaction was stopped by adding 25 μL of 100% TCA (trichloroacetic acid). As for C281W/M362T AADC is incubated at 10 μM protein concentration with 2 mM L-Dopa in 100 mM potassium phosphate buffer, pH 7.4 at 25 °C. Concentration-time curves were followed by withdrawing aliquots of 225 μL at time intervals and quenching the reaction by adding 25 μL of 100% vol/vol TCA. Proteins were then precipitated on ice and removed by centrifugation. Supernatants were analyzed by HPLC as described [16] using a Gemini C18 column (150 × 4.6 mm, Phenomenex, CA, USA) and performed on a Jasco PU-2080 Plus HPLC system equipped with a UV-1570 detector set at 295 nm. Samples were eluted in 50 mM potassium phosphate, pH 2.35, at a flow rate of 1 mL/min. Standard curves of peak area as a function of coenzyme or dopamine concentrations were prepared with commercially available PLP and dopamine and appropriately quantified.

2.8. Spectroscopic measurements

Far-UV circular dichroism (CD) measurements were acquired in 58 mM potassium phosphate buffer, pH 7.4, at 25 °C at a scan speed of 50 nm/min with a bandwidth of 2 nm at 2 μM protein concentration and 10 μM PLP for the holoenzymes. Thermostability was determined by monitoring the CD signal at 222 nm of 2 μM enzyme on a 25–90 °C linear temperature gradient, with a temperature slope of 1 °C/min. Near-UV CD measurements were performed in 100 mM potassium phosphate buffer pH 7.4 at 25 °C at 5 μM protein concentration and 10 μM PLP for the holoenzymes. All spectral measurements were recorded with a Jasco J-710 spectropolarimeter.

2.9. Patients consents

The present study has been approved by the local ethic committees (Ethics Committee of the Medical Faculty, University of Heidelberg, Germany under the document identifiers S-533/2015 and S-471/2014, and Ethics Committee of Sapienza University of Rome with signed informal consent).

2.10. Bioinformatics analyses

Human AADC sequence was aligned with 75 homologues sequences retrieved from Uniref-90 database by the homolog search algorithm PSI-BLAST and aligned using Multiple Sequence Alignment software CLUSTALW on ConSurf server (http://consurf.tau.ac.il). A conservation score (9 = highly conserved, 1 = highly variable) was attributed to each residue. Structural analysis and *in silico* mutagenesis of the pig DDC (PDB: 1JS6; ~90% sequence identity with the human homologous) was carried out using Pymol 2.0 (The PyMOL Molecular Graphics System, Version 2.0 Schrödinger, LLC.).

2.11. Determination of solubility level of the C281W, M362T and C281W/M362T AADC variants

E. coli has been used as a model for the expression study of pathogenic AADC variants. Chemically competent bacteria were transformed with the mutagenized plasmids as described in the expression and purification section. Cultures were grown in the absence or presence of 50 μM exogenous PLP and 1 mL of each culture was processed following the procedure described above. After lysis, samples were treated with DNAse (10 U) at room temperature for 30 min. The whole extract was separated by centrifugation at 13,200 rpm, 10 min, 4 °C. Total protein content in the crude lysate was quantified and 15 μg of total protein was run on a 12% (*w*/w) SDS-PAGE gel. Proteins were transferred from the gel on a nitrocellulose membrane by a Mini Trans-Blot cell (BioRad). Membranes were blocked with a 5% (w/w) milk solution at 37 °C for 1 h and, after washing, incubated with a 1:200 (*v*/v) diluted anti-AADC monoclonal antibody solution overnight at 4 °C. The membranes were washed and incubated with a 1:4000 (v/v) anti-mouse secondary antibody solution for 1 h at 25 °C. Blotted proteins were detected and quantified with Immobilon Western Chemiluminescent HRP Substrate (Merck-Millipore) using the ChemiDoc XRS Imaging System (Bio-Rad, Hercules, CA). Bands were quantified using ImageJ software (Fiji).

2.12. Mass protein determination

The mass of the samples was assessed by mass spectrometry using a Xevo® G2-XS ESI-Q-TOF mass spectrometer (Waters Corporation, Milford, Massachusetts, USA). Measurements were conducted in positive mode. The capillary potential was set at 1.5 kV. The source temperature was at 100 °C. Mass values were determined at a resolution >35.000 and an accuracy <5 ppm. Mass spectra were analyzed using MassLynx 4.1 software (Waters). All samples were desalted by RP-HPLC before loading onto the mass spectrometer. The analysis was carried out on a 1200 series Agilent Technologies (Santa Clara, California, USA), with a Jupiter C4 column (4.6 mm × 250 mm, 5 μm; Phenomenex, CA, USA) eluted with the gradient of water and acetonitrile, containing 0.1% of trifluoroacetic acid, from 5 to 38% in 5 min and from 38 to 43% in 15 min at a wavelength of 226 nm.

3. Results

3.1. Clinical presentation of the patients involved in this study

Table 1 reports the patients involved in this study together with the amino acid substitution and genotype presentation of the genetic alteration. Patient 1 (previously referred as patient 3 [17], c.206C>T g.50540024G>A, homozygous T69M variant) is a now 20-year-old young man, suffering from AADC deficiency, whose metabolic markers profile is shown in Table 2. He was born at term after uneventful pregnancy. Early postnatal development was normal until he became apparent with a hypotonic muscle tone at the age of 3 months. Motor milestones were achieved with delay, *e.g.* the ability to sit with 18 months and ambulatory walking with 3 years. Speech development

Table 1
Patients involved in this study.

#	Reference	Genotype	Amino acid substitutions	Pediatric Neurotransmitter Disorders db	ClinVar db
Patient 1	Patient 3 in [17]	c.206C>T g.50540024G>A; c.206C>T g.50540024G>A	T69M/T69M	BIOMDB312 (T69M)	VCV001057684
Patient 2	Patient 6 in [17]	c.206C>T g.50540024G>A; c.439A>C g.50529339T>G	T69M/S147R	BIOMDB312(T69M) BIOMDB220(S147R)	VCV001057684 VCV000017812
Patient 3	new	c.843C>G g.50499181G>C; c.1085T>C g.50470128A>G	C281W/M362T	BIOMDB425(C281W) BIOMDB424 (M362T)	-- --

db = database.

Table 2
Clinical data update, metabolic markers and genetic analyses of Patient 1, homozygous T69M, and Patient 2, compound heterozygous T69M/S147R, involved in this study.

	Patient 1[a]	Patient 2[b]
Sex	male	female
Age	20	30
Birth weight (in g)	2935	1920
Age at diagnosis (in months)	70	57
Age at 3-OMD DBS measurement	19	18
DBS 3-OMD (Ref. < 3 μmol/l)	1.9	3.16
CSF 3-OMD (Ref. 0–128 nmol/l)	655	736
CSF HVA (Ref. 427–989 nmol/l)	80	35
CSF HIAA (Ref. 159–528 nmol/l)	11	0
L-Dopa (0–15 nmol/l)	655	–
L-5-HTP (0–20 nmol/l)	115	–
AADC enzyme activity (Ref. 47–119 pmol/ml/min)	1	<0

[a] Patient 3 in [17].
[b] Patient 6 in [17]; 5HIAA, 5-hydroxyindoleacetic acid; HVA, homovanillic acid; 3-OMD, 3-*O*-Methyldopa; L-5-HTP, L-5-hydroxytryptophan.

was also delayed. Today, at the age of 20 years, the patient is able to walk although partly clumsy without difficulties. He shows reduced fluidity of fine motor movements, but no signs of dystonia. He presents with a prominent language development disability with phonetic-phonological disorder, marked dysgrammatism, limited active vocabulary, and markedly reduced language comprehension skills with underlying mental retardation (Full Scale IQ 55). The current medical regimen consists of bromocriptin (0.5 mg/kg/d), selegiline (0.3 mg/kg/d) and rotigotine (4 mg/d). In summary, his clinical course can be described as a milder phenotype with little movement disorder and largely preserved functionality in daily life.

AADC deficiency Patient 2 (previously referred as patient 6 [17], c.206C>T g.50540024G>A and c.439A>C g.50529339T>G, compound heterozygous T69M/S147R variant) is a now 30-year-old young woman (Table 2). She presented oculogyric crisis at the age of 4 months as first clinical symptoms after unremarkable dizygotic twin pregnancy. She failed to achieve developmental milestones and today presents with fixated right sided torticollis, truncal hypotonia and dystonic posturing of all extremities. The ankle joints of both legs are contract with spastic supination. Her spine shows a severe S-shaped-scoliosis configuration, both hip joints are luxated, and the patient is completely bedridden. Impairment of shoulder and neck muscles led to severe dysphagia, which resulted in severe weight loss (currently 26.6 kg, SDS -7.55). No voluntary use of the upper and lower extremities is possible. Recently, she was diagnosed with a neurogenic bladder disorder. The current medication regimen consists of a combination of bromocriptine (0.65 mg/kg), rotigotine (4 mg/d) and selegiline (0.45 mg/kg/d). To counteract dystonic crises, the patient also receives lorazepam (1 mg) as needed. Her disease course can be described as a severe form of AADC deficiency.

Patient 3 is a new compound heterozygous patient (c.843C>G g.50499181G>C and c.1085T>C g.50470128A>G). This 16-year-old male was born from non-consanguineous Italian parents after normal pregnancy and delivery. Perinatal history was unremarkable. A relevant axial hypotonia detected since the birth was the anticipatory feature of a delay in motor developmental (head control: 9 months; trunk control: 12 months; unsupported gait: 3 years) with severe speech impairment and absence of utterance of articulate sounds. In contrast the development of social interaction, language comprehension, and cognitive skills was relatively preserved.

At the age of 4 months, he presented with an episode of stupor after a prolonged fasting state associated to an intercurrent febrile event. In the following years recurrent relapses characterized by gait instability and action tremor were triggered by protracted fast status, also beyond the occurrence of febrile events. These symptoms remitted with the normalization of nutritional supply. Since the age of 3 the patient underwent repeated gastroenterological evaluation because of a chronic diarrhea (including non-digested foods in the stools). Oculogyric crises emerged at the age of 3 years.

On examination, when 6 years old, he exhibited: elongated face with hypotelorism (Fig. 2S), micrognathia and severely arched palate, anarthria with incessant drooling without dysphagia, exotropia of the right eye with impaired binocular fusion and alternate fixation, a generalized bradykinesia, hypotonia and clumsiness, autonomous gait with an enlarged basis, mild dysmetria and dis-diadochokinesia of limbs, and orthostatic hypotension.

A mild increase of plasma prolactin (61.5 ng/ml; reference range 2–19.50 ng/ml) led to CSF examination, which disclosed a pattern of alteration in biogenic amine metabolites compatible with the diagnosis of AADC deficiency. AADC enzyme activity was severely reduced (Table 3). Sanger sequencing of all exons and exon-intron regions of the *DDC* (reference ENSG00000132437.1) revealed compound heterozygosity for the two variants C281W/M362T, inherited by the mother and the father, respectively. According to the mutation prediction programs SIFT (v6.2.0) and MutationTaster (v2013), the two variants are deleterious and disease causing, respectively, so supporting the pathogenicity of the genotype.

After the diagnosis, bromocriptine was gradually introduced (up to 7.5 mg in 3 daily administrations) with disappearance of the oculogyric crises and stabilization of clinical status. The patient continued to complain of bradykinesia, asthenia and fatigability associated to daily on-off phenomena. At the age of 14 the occurrence of a remarkable clinical worsening leaded to a further assessment of CSF neurotransmitters, which showed a decline of homovanillic acid, 5-hydroxyindoleacetic acid, with a still high level of 3-*O*-methyldopa (Table 3). Drooling remained an extremely disabling problem with relevant social impact. At the age of 15 he was a good mood optimistic boy with anarthria but excellent gestural language, moderate intellectual disability (Wechsler Intelligence Scale for Children-IV edition: Full Scale IQ = 40; Verbal Comprehension Index =54; Perceptual Reasoning Index =48, Working Memory Index = 49; Processing Speed Index = 50), and brilliant social adaptive skills with the best results on abilities concerning daily activities and socialization (Vineland Adaptive Behavior Scales II edition: Communication Domain = 59; Daily Living Skills Domain = 89; Socialization Domain = 71; Composite Score = 71).

Bromocriptine was replaced by transdermal rotigotine (up to 6 mg/day) that resulted in disappearance of on-off phenomena and fluctuating weakness, and improvement of bradykinesia, drooling, motor coordination and initiative, and mood. UPDRS-part III scores confirmed an improvement involving lower limb rigidity (0 *versus* 1 for both sides) and agility (1 *versus* 3 for both sides) after the introduction of rotigotine.

Table 3
Metabolic markers of compound heterozygous Patient 3 (C281W/M362T).

CSF BIOGENIC AMINE AND PTERIN METABOLITES	VALUES AT THE AGE OF 6 YEARS	REFERENCE RANGE (at the age of 6 years; nmol/L)	VALUES AT THE AGE OF 14 YEARS	REFERENCE RANGE (at the age of 14 years; nmol/L)
5HIAA	21.6 nmol/L	88–178	7 nmol/L	68–115
HVA	85.1 nmol/L	144–801	25 nmol/L	148–434
HVA/5HIAA	3.9	1.5–3.5	3.5	1.5–3.5
3OMD	1720.0 nmol/L	<50	270 nmol/L	<50
L-5-HTP	101.3 nmol/L	<10	32 nmol/L	<10
Neopterin	10.2 nmol/L	9–20	Not performed	–
Biopterin	23.7 nmol/L	10–30	Not performed	–
%Biopterin	69.9	53–60	Not performed	–
AADC enzyme activity: (Reference Range 36–129 pmol/min/ml) 4 pmol/min/ml				

5HIAA, 5-hydroxyindoleacetic acid; HVA, homovanillic acid; 3OMD, 3-*O*-Methyldopa; L-5-HTP, L-5-hydroxytryptophan; %Biopterin, 100 x [Biopterin]/ [Neopterin] + [Biopterin].

At the age of 16 a more stable clinical condition was obtained by adding selegiline (up to 5 mg/day) and pyridoxine (up to 300 mg/day).

3.2. The heterodimer T69M/S147R is produced in high yields and displays higher stability and reduced activity than expected

Having demonstrated (Supplemental Results) that both monomers of WT AADC give rise in any combination to closely identical proteins (Table 4), we used this approach for generating heterodimers deriving from different mutations in the two alleles. In particular, we produced His-tagged variant homodimers and compared them to the related His-tagged WT, while double tagged variant heterodimers were compared to the His/StrepWT.

At first, we addressed the biochemical characterization of the compound heterozygous phenotype T69M/S147R, since some of the structural and kinetic features of the two related homodimers have been already measured in previous papers [3,18]. In those studies it has been reported that the T69M homodimer presents a k_{cat} value 46% compared to that of the WT enzyme, while both K_m and the equilibrium dissociation constant for PLP, $K_{D(PLP)}$, are slightly affected [3]. In addition, S147R homodimer [18] results strongly affected in k_{cat} (0.1% with respect to the WT), while its K_m is almost unaffected and the affinity for the coenzyme highly compromised.

The expression of the T69M/S147R heterodimeric variant presents a good yield (5–6 mg/l) similar to that of the double-tagged WT evidencing that the combination of the substitutions has not influenced protein expression. Western blot (WB) analysis confirmed the presence of both tags in the purified heterodimeric form (Fig. 5S). Notably, this is the first time for AADC that an optimal yield of heterodimeric species has been obtained.

The two homodimers and the heterodimer present identical far UV CD signals (data not shown) and near UV and visible CD bands comparable to the corresponding ones of the related WT species both in the holo and in the apo state (Fig. 1) revealing the absence of differences in the global folding unless subtle alterations in the orientation of the aromatic amino acids in the variants, as shown by the slightly decreased bands at 280 nm in their holo form with respect to the WT species. Thermostability of the three species is reported in Table 5. We found that the apo form of the heterodimer has a melting temperature (Tm) reduced by 1.81 °C compared to the WT. The two apo homodimeric variants show a Tm reduction by 1.47 °C for T69M and 4.82 °C for S147R compared to the WT. Thus, the concurrent presence of the two mutations helps to maintain stability. As for the holo forms, the Tm for the heterodimeric species is 1.16 °C lower than the corresponding WT and reaches approximately the average value between the two homodimers (ΔTm of −0.76 °C for T69M and 1.53 °C for S147R), confirming that the heterodimer is a stable species, even more than the S147R homodimer.

This behavior is also mirrored by the equilibrium dissociation constant for PLP that results to be 310 ± 30 nM for T69M/S147R variant (about 3.9 times higher than the corresponding one for WT), whereas T69M has a $K_{D(PLP)}$ of 100 ± 13 nM [3] and S147R of 846 ± 63 nM [18], equal and 8.5 higher with respect to the WT, respectively. This could be interpreted as a positive complementation in PLP equilibrium binding for the heterodimer.

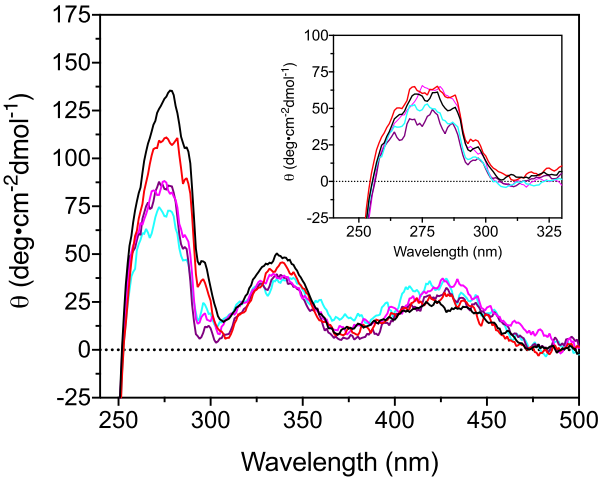

Fig. 1. Near UV CD spectra of holo and apo HisT69M, HisS147R and His/Strep T69M/S147R AADC.
The holo near UV and visible spectra of 1 mg/ml HisWT (black), His/StrepWT (red), HisT69M (magenta), HisS147R (cyan) and Strep/HisT69M/S147R (fuchsia) are recorded in 100 mM potassium phosphate buffer at pH 7.4. Inset: spectra of the corresponding apo forms in the same color code as above.

Table 4
Kinetic parameters for L-Dopa decarboxylation by differently tagged WT AADCs.

WT AADC	k_{cat} (s^{-1})	K_m (mM)	k_{cat}/K_m (s^{-1} mM^{-1})
His-tag[a]	7.6 ± 0.1	0.11 ± 0.01	69 ± 6
Strep-tag	5.3 ± 0.2	0.13 ± 0.02	41 ± 6
His-Strep-tag	6.3 ± 0.1	0.14 ± 0.02	45 ± 7

[a] From [3].

Table 5
Thermostability at 222 nm of the different enzymatic species of the compound heterozygous T69M/S147R and C281W/M362T AADC.

AADC species	Tm (apo) °C	Tm (holo) °C
HisWT	64.80 ± 0.03	67.1 ± 0.1
His/StrepWT	64.27 ± 0.03	67.86 ± 0.03
HisT69M	63.33 ± 0.02	67.55 ± 0.02
HisS147R	59.98 ± 0.02	65.57 ± 0.02
Strep/HisT69M/S147R	62.46 ± 0.02	66.70 ± 0.02
HisM362T	59.89 ± 0.02	67.54 ± 0.02
Strep/HisC281W/M362T	60.34 ± 0.06	62.27 ± 0.07

Enzyme activity was too low to be measured by the conventional spectrophotometric assay. Using HPLC (see Materials and Methods) we determined the amount of dopamine produced at L-Dopa concentrations up to 8 mM without still reaching saturation (Fig. 6S). Thus, only the catalytic efficiency value, k_{cat}/K_m, could be obtained and compared to those of the already characterized T69M and S147R variants [3,18] and with the respective WT reference species (Table 4). While T69M and S147R have a catalytic efficiency of about 11% and 0.001%, respectively, in comparison to the WT, the heterodimer T69M/S147R has a k_{cat}/K_m of 0.080 ± 0.003 s^{-1} mM^{-1}, a value that is 0.18% that of the double tagged WT (Table 4). This suggests a negative complementation in terms of activity, despite the structural stability of this variant is higher than the average of the single homodimers. A bioinformatic analysis could support the obtained results. Since the bioinformatic analyses of the amino acid substitutions for the two homodimers T69M and S147R have been already performed [3,18], we carried out an investigation on the heterodimeric protein. As shown in Fig. 2, both substituted residues are located at the dimer interface. However, in the heterodimeric state, they are spatially separated one from each other. Thr69 is in the proximity but outside of the active site and its substitution to methionine abolishes the interface contact with Ala106 and might slightly alter the active site of one subunit, by perturbing the position of key residues of the important structural element loop1, such as Phe76 and Trp71, without any influence on the second active site. S147R on the adjacent monomer is one of the residues identified to be critical in Fold-type I PLP-enzymes for the phosphate binding "cup" of the coenzyme [19] and thus it is responsible for the low PLP affinity of the subunit carrying the substitution. The bulky side chain of Arg147 could directly affect the conformation of the loop 3 of the neighboring subunit and the network of polar interactions between the active sites (Fig. 2). These interactions involve the structural element loop3 of both monomers and several water molecules at the dimer interface between the active sites. The induced perturbation could lower the activity of both of them since loop 3 is an essential structural element for proper enzymatic function [4,5]. Thus, the less severe enzymatic phenotype of T69M with respect to S147R and T69M/S147R is understandable. The heterodimer T69M/S147R results instead less affected in structure showing at least one nearly well-structured active site, particularly in terms of PLP binding (that of the chain with T69M), that is not sufficient to rescue the enzymatic activity. This is in fact strongly influenced on both the active sites by alterations directly (on its active site) or indirectly (on the neighboring active site) by a single S147R substitution. The very modest activity of S147R homodimer is explained by the huge effect determined on both active sites by the mutation.

Following this view, it can be understood the mild clinical phenotype reported for homozygous patient 1 carrying the T69M alteration [17] and the more severe clinical traits exhibited by the compound heterozygous patient 2 [17].

3.3. The heterodimer C281W/M362T is expressed despite the low expression of the homodimer C281W and displays discrete activity and retained structural requirements

C281W and M362T homodimers are both expressed in the soluble fraction of bacterial lysates. In contrast to T69M and S147R which were recovered in good yields in the soluble fraction, the amounts of C281W and M362T are 35% and 89% of the WT after 2 h induction and a further drop to 9% and 20% after overnight induction (Fig. 3). Notably, the insoluble fraction revealed the presence of all species, confirming that the impairment is not due to expression but to solubility. Thus, we decided to shorten the induction time to 2 h. While M362T was recovered in amounts similar to those of the WT, C281W was obtained in amounts less than 0.01%, that preventing its further characterization. The double tagged heterodimer StrepC281W/HisM362T was recovered in amounts of about 0.5–1% in the soluble fraction and purified as reported in the Materials and Methods section. To control for the influence of the tag on solubility, M362T was cloned with the Strep-tag-II and the heterodimer produced with inverted tags (HisC281W/StrepM362T) with no differences in solubility pattern. WB analysis confirmed the presence of both tags in the purified heterodimeric form (Fig. 5S). In addition, StrepC281W homodimer was recovered predominantly in the insoluble fraction as seen for HisC281W homodimer (data not shown).

The far UV CD spectra of M362T and C281W/M362T species are superimposable with that of the WT (data not shown), suggesting that the secondary structure is preserved. However, the thermostability at 222 nm shows that the ΔTm value WT-M362T is 4.91 °C in the apo form and almost identical in the holo form, while the ΔTm value of double tagged WT-C281W/M362T is 3.93 °C in the apo form and 5.59 °C in the holo form (Table 5). This suggests that the variant heterodimer is less stable than the variant homodimer compared to the WT in the holo form, whereas both apo species are less stable than the corresponding WT forms.

The near UV CD signals of both the holo species M362T and C281W/M362T exhibit a decrease in the aromatic bands of 50% and about 45%, respectively (Fig. 4a), while the apo dichroic signals of M362T are superimposable to those of the WT (inset Fig. 4a). Overall, these changes could be related to a change in the asymmetry of aromatic amino acids. Notably, the intrinsic fluorescence bands are, instead, superimposable (Fig. 4b), arguing that the observed changes are due to subtle

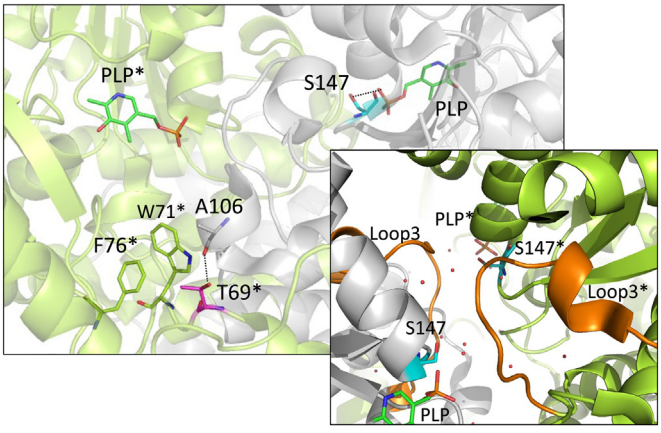

Fig. 2. Relative position of Thr69 and Ser147 residues.
Ribbon representation of the AADC dimer (pdb file 1JS6). The two monomers are colored grey and green, respectively. Thr69 and Ser147 are represented as magenta and cyan sticks, respectively. Zoomed panel indicates the relative position of Ser147, loops 3 and PLP molecules on the AADC dimeric structure. Water molecules are represented as red spheres. * denotes residues belonging to the green subunit.

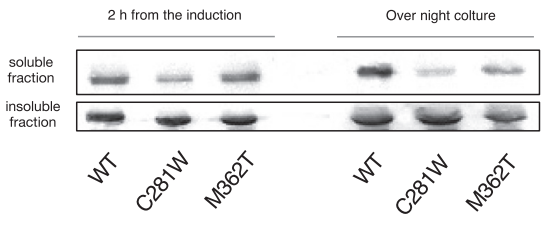

Fig. 3. Expression of HisC281W and HisM362T homodimers and of the His/StrepC281W/M362T heterodimer after induction.
Soluble and insoluble fractions of C281W and M362T homodimers revealed by WB after 2 h and overnight induction. Western blot analysis is performed with 15 μg of total protein content from soluble lysates of *E. coli* loaded on 12% acrylamide gel. Determination of the expression levels of each variant was estimated using ImageJ software (Fiji) and is reported in the text as percentage with respect to the WT.

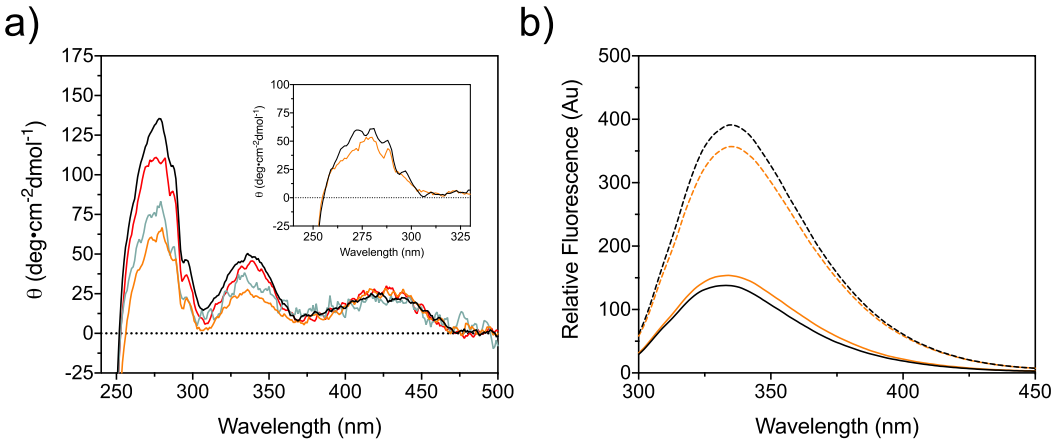

Fig. 4. Near UV and visible CD and intrinsic fluorescence spectra of holoM362T and C281W/M362T.
The holo near UV and visible spectra of 1 mg/ml HisWT (black), His/StrepWT (red), M362T (yellow) and C281W/M362T (green) are recorded in 100 mM potassium phosphate buffer at pH 7.4. Inset: spectra of the WT and M362T apo forms in the same color code as above (a). Holo WT (black straight line) and M362T (yellow straight line) at 1 μM concentration in 100 mM potassium phosphate buffer, pH 7.4 have been excited at 280 nm and the emission spectra have been collected. Apo species (dotted line) excited under the same experimental conditions (colors as for the holo counterpart) (b).

modifications induced by the amino acidic substitution. In addition, the dichroic visible signals associated to PLP are modified in both variants suggesting an alteration in the coenzyme binding site mirrored by the measured $K_{D(PLP)}$ that resulted 271 ± 20 nM for M362T and 1232 ± 319 nM for C281W/M362T. These values are 2.7-fold and 11.2-fold higher than the $K_{D(PLP)}$ of the corresponding tagged WT species.

Kinetic parameters of M362T are slightly altered, k_{cat} maintains a value of about 60% with respect to that of the WT and K_m increases by a factor of 1.6 determining a 35% of catalytic efficiency. The heterodimer, instead, shows an invariant K_m but a decreased k_{cat} that is 29% that of the WT (Table 6) determining a catalytic efficiency about 34% compared to the WT.

Due to the failure to obtain purified C281W, we could not assess the C281W/M362T heterodimer in terms of complementation. Nevertheless, it is striking that we were able to obtain the heterodimer, albeit in small amounts, but the homodimeric C281W was not soluble enough to be purified.

A bioinformatic analysis of the protein regions altered by mutations can help us to decipher data obtained in solution. Met362 belongs to the helix 358–369, a region on the edge of large and C-terminal domains and close to the N-terminal domain of the neighboring monomer (Fig. 5). The residue is immersed into a hydrophobic cleft and is surrounded by apolar residues (Met118, Leu122, Ile144, Leu305, Val307, Phe366). The cavity is protected from the solvent exposition mainly by the salt bridge between the Glu283 and the Arg379 side chains and by a polar contact involving the Gln375 side chain and the Ile280 backbone. The Cys281 residue locates in the same hydrophobic region (Fig. 5) quite close to the Glu283-Arg379 "lock". The Cys side chain is placed into a hydrophobic environment and is not engaged in any polar contact. Thus, the contact with Arg379 is a common element that implicates both Met362 and Cys281.

From the conservation analysis performed by Consurf Server, although Met362 resulted poor conserved, only apolar amino acids were found in the corresponding position in homologous proteins (Ile, Leu, Val, Met). These data remark the strictly apolar character of the Met362 microenvironment. On the contrary, Cys281 resulted highly conserved and no alternative residues were identified by the multiple sequence alignment (see Material and Methods). The substitution Met362 to Thr does not increase the hindrance of the residue but introduces a polar side chain into a hydrophobic environment. Considering that the de-solvatation free energy of a Thr residue is ~5 fold higher than that of a Met residue [20,21], a Met-to-Thr exchange is expected to alter the normal protein folding by promoting alternative folding pathways. On this basis, it is reasonable to suggest that the M362T substitution could affect the local conformation causing a possible slight misfolding defect.

Cys281 to Trp substitution is expected to generate a massive steric hindrance in proximity of the junction between the helices 282–288 (large domain) and 372–395 (C-terminal domain). At local level the *in silico* mutagenesis suggested that the substitution could (i) expose the large hydrophobic side chain of the Trp to the solvent and (ii) affect the Glu283-Arg379 salt bridge with the possible exposition of several hydrophobic residues to the polar environment. Both effects determine alterations of the local conformation leading to possible unstable and/or insoluble folding products. For these reasons, C281W substitution is predicted to generate a folding defective variant and following this view, we could interpret the impossibility to obtain it in the soluble fraction in amounts sufficient to be purified.

In the heterodimer one subunit has Met362 exchanged with Thr causing local effects mildly reflected in the Glu283-Arg379 salt bridge that is maintained by an unaltered bond network involving intact Cys281. The other subunit, carrying the C281W mutation, could experience a more dramatic disassembling, minimized by a sufficient integrity in the cognate M362T subunit.

Thus, bioinformatic analyses suggest that both alterations lead to impaired folding with C281W substitution resulting in a more severe impairment and found mainly insoluble. M362T can fold giving rise to a species with some structural defects underlined by measured lower apo Tm or affinity for the coenzyme, with overall good catalytic competence since the protein regions responsible for catalysis are unaffected by mutation. The good performing M362T subunit should in some manner trigger the folding/assembly of C281W chain in the heterodimeric species.

Table 6
Kinetic parameters for L-Dopa decarboxylation by M362T and C281W/M362T.

AADC species	k_{cat} (s^{-1})	K_m (mM)	k_{cat}/K_m (s^{-1} mM^{-1})
M362T	4.6 ± 0.2	0.18 ± 0.06	25 ± 8
C281W/M362T	1.8 ± 0.1	0.13 ± 0.04	14.0 ± 0.4

4. Discussion

Unraveling of the enzymatic properties of heterodimeric AADC protein variants could represent a basis to understand the wide spectrum of clinical phenotypes of patients who are compound heterozygotes for

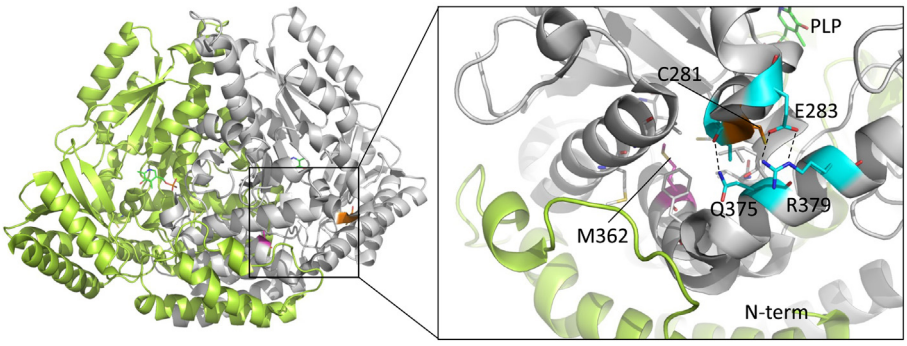

Fig. 5. Structural location and microenvironment of Cys281 and Met362 residues.
Ribbon representation of the AADC dimer (pdb file 1JS6). The two monomers are colored grey and green, respectively. The zoomed panel indicates the position of Cys281(orange), Met362 (magenta), Glu283(cyan), Arg379(cyan) and Gln375(cyan). Residues belonging to the hydrophobic cleft are represented as grey sticks.

DDC gene. Indeed, they can theoretically express both homodimers and the heterodimer as well, with relevant variability in the resultant enzymatic activity.

Here, we have had the unprecedent opportunity to explore structural and functional protein features associated with two compound heterozygous *DDC* genotypes and to correlate them with the related phenotypes, their clinical data and their drug treatments.

In literature, only for human phenylalanine hydroxylase such a deep investigation on compound heterozygosis patients, involving great number of mutations and genotypes, has been carried out leading to advances in the knowledge of genotype-phenotype correlation [8,22–24] and to the possibility of elucidating the molecular basis for tetrahydrobiopterin responsiveness evidencing the role of subunit interactions in conformational corrections determined by the substrate and response to the cofactor [8].

The strategy employed here to clone with pETDuet-1 vector and express heterodimers in high yields and quick times, allowed us to characterize two AADC heterodimeric variants never analyzed before: T69M/S147R and C281W/M362T. The mutation sites are spread in different domains of the AADC protein: from the N-terminal domain to the large domain up to the C-terminal domain. In addition, we have also characterized the related homodimeric proteins to understand how data collected with heterodimers could be interpreted in terms of allele dominance or chemical substitution severity or protein region modification.

While the S147R substitution has been observed only in heterozygosis [17], homozygous T69M gives rise to a homodimeric variant [3,17] that retains 10% of the WT catalytic efficiency [3]. The S147R homodimeric AADC appears to be structurally more affected (lower Tm and higher $K_{D(PLP)}$) and only achieves a modest catalytic efficiency compared to the WT [18]. Most of the properties of T69M/S147R AADC are related to the severity of S147R substitution that, as bioinformatic and structural analyses suggest, affects not only its active site but also the active site of the neighboring subunit. This helps to understand the functional impact and lower activity measured for the heterodimer compared to the T69M homodimer. Interestingly, as far as thermal stability and equilibrium dissociation constant for PLP are concerned, a positive effect is observable arguing that 1) a more stable protein does not necessarily correlate with residual activity, and 2) the presence of the milder T69M substitution attenuates the strong impact of the severe S147R on enzymatic properties. The clinical phenotypes, re-evaluated 10 years after the first publication of these individuals [17], are in accordance with the *in vitro* and *in silico* data, as patient 1 harboring the T69M substitution suffers from a milder clinical phenotype compared to the compound heterozygous patient 2.

A previously unreported compound heterozygous patient 3 led us to investigate the two homodimers and the heterodimer responsible for the clinical phenotype. Cys-281 is part of a protein region essential for folding [5] which might explain the difficulty to recover it in the soluble phase. It has been already reported that variants mapping in this protein region, so far characterized, exhibited solubility/folding troubles retaining good activity if they succeed in being stabilized enough [5]. In addition, Met362 at the beginning of the C-terminal domain also contributes to lock the protein in a conformation that, if altered, could lead to impaired folding. This might explain the reduced stability of apoM362T and of both apo and holo C281W/M362T. This effect is underlined by altered spectroscopic signals and a decreased affinity for the coenzyme (2.7-fold and 12.3-fold for M362T and C281W/M362T, respectively). Interestingly, these structural defects do not lead to catalytic impairments similar to T69M/S147R, since the active sites appear uncompromised. Again, this observation correlates with higher plasma activity of AADC measured by clinical analyses of the heterozygous patient 3 (Table 3) when compared to both patient 1 and patient 2 (Table 2). This brings us to the conclusion that if a structural defect directly affects the active site, it will cause a worse functional damage than that caused by a variant affecting folding. Moreover, due to impaired folding of C281W, it is possible that the enzymatic pool of patient 3 is mainly composed of the M362T homodimer which has been shown to have higher activity than both the heterodimer (and the T69M homodimer) further explaining the plasma activity of AADC.

The overall drug treatment of the heterozygous patients was similar. Patient 3 receives additional pyridoxine to stabilize protein folding and/or exert a chaperon effect as in [25]. Based on our investigations, we propose that pyridoxine could be of less help for patient 2 since one active site is compromised and the other is also affected through the loop3 element, necessary for catalytic activity.

In order to possibly find a rationale for the effects displayed by the heterodimeric enzymes, it seems that one hallmark to predict positive or negative complementation for AADC activity could be related to the impact of the amino acid substitutions on both active sites. It is interesting that T69M/S147R exerts negative complementation effects as A91V/C410G [7] whose effects were attributed to damages on both active sites. In contrast, R347Q/R358H [6] exhibits a positive complementation and only one active site seems to be compromised. We compared k_{cat} values (as markers of good or bad catalytic competence) with the severity of the reported disease course. The catalytic constants of the heterodimeric species range from 4 to 29% compared to the WT. In more depth, the value of k_{cat} decreases from C281W/M362T (1.8 s^{-1}) to R347Q/R358H (0.45 s^{-1}) to A91V/C410G (0.38 s^{-1}) to T69M/S147R (0.27 s^{-1}). However, looking at heterodimer structural signals, such as $K_{D(PLP)}$, it seems that R347Q/R358H [26] and T69M/S147R display a slight increase in such constant compared to the WT, while C281W/M362T and (as the prediction deduced from two homodimeric values) also A91V/C410G [7] possess a much higher $K_{D(PLP)}$. This underlines a possible difficulty of these variants to bind the coenzyme in the absence of external supply. A prediction of clinical outcome is therefore

difficult, since there is an apparent divergence among functional data and structural signals. The clinical constellation of compound heterozygous patients reveals that a heterozygous patient bearing R347Q/R358H modifications [26] and patient 2 of the present investigation are affected by a severe form of AADC deficiency [2], while the patient bearing the A91V/C410G modification [7] and patient 3 of the present investigation can be considered as mild cases. A discrepancy between biochemical observation of the heterodimer and the extent of clinical symptoms of heterozygous patients could be reasonably based on the expression of the related homodimers in patients. It seems that for AADC deficiency, 1) positive or negative complementation, and 2) residual function of each of the homodimers representing a significant fraction in the AADC protein population must be considered. If one homodimer is highly compromised, the clinical phenotype is severe even if the heterodimer shows positive complementation in enzymatic activity and/or structural signals. In addition, variants with high influence on folding problems, resulting in poor solubility, could exert a high influence on the ratio of allele combinations relatively expressed in patients and thus on the relative abundance of homo and heterodimers.

Overall, the combination of *in vitro* experiments with recombinant proteins, *in silico* bioinformatic analyses and the assessment of *in vivo* clinical data allows us to integrate multi-dimensional knowledge and paves the way to understand how allele dominance is governed in AADC deficiency.

Funding

This work was possible thanks to grants from AADC Research Trust, United Kingdom/PTC-Therapeutics, United States and FUR-University of Verona, Italy to MB.

Acknowledgments

We acknowledge Simona Orcesi MD, Neurological Institute IRCSS Mondino Foundation,Unit of Child Neurology and Psychiatry, Pavia, Italy, and Beat Thöny, Division of Metabolis, Department of Pediatrics, University of Zürich, Switzerland, for diagnostic work-up and follow-up. The skillful technical assistance of Silvia Bianconi and Dr. Raffaella Pacchiana, Department of Neuroscience, Biomedicine and Movement Sciences, University of Verona, Italy, is also gratefully acknowledged.

We thank the patients and their parents for participation in the iNTD registry study.

Appendix A. Supplementary data

Supplementary data to this article can be found online at https://doi.org/10.1016/j.ymgme.2021.08.011.

References

[1] N. Himmelreich, R. Montioli, M. Bertoldi, C. Carducci, V. Leuzzi, C. Gemperle, T. Berner, K. Hyland, B. Thöny, G.F. Hoffmann, C.B. Voltattorni, N. Blau, Aromatic amino acid decarboxylase deficiency: molecular and metabolic basis and therapeutic outlook, Mol. Genet. Metab. 127 (2019) 12–22.

[2] T. Wassenberg, M. Molero-Luis, K. Jeltsch, G.F. Hoffmann, B. Assmann, N. Blau, A. Garcia-Cazorla, R. Artuch, R. Pons, T.S. Pearson, V. Leuzzi, M. Mastrangelo, P.L. Pearl, W.T. Lee, M.A. Kurian, S. Heales, L. Flint, M. Verbeek, M. Willemsen, T. Opladen, deficiency, Consensus guideline for the diagnosis and treatment of aromatic l-amino acid decarboxylase (AADC), Orphanet J Rare Dis 12 (2017) 12.

[3] R. Montioli, M. Dindo, A. Giorgetti, S. Piccoli, B. Cellini, C.B. Voltattorni, A comprehensive picture of the mutations associated with aromatic amino acid decarboxylase deficiency: from molecular mechanisms to therapy implications, Hum. Mol. Genet. 23 (2014) 5429–5440.

[4] R. Montioli, A. Paiardini, M.A. Kurian, M. Dindo, G. Rossignoli, S.J.R. Heales, S. Pope, C.B. Voltattorni, M. Bertoldi, The novel R347g pathogenic mutation of aromatic amino acid decarboxylase provides additional molecular insights into enzyme catalysis and deficiency, Biochim. Biophys. Acta 1864 (2016) 676–682.

[5] R. Montioli, G. Bisello, M. Dindo, G. Rossignoli, C.B. Voltattorni, M. Bertoldi, New variants of AADC deficiency expand the knowledge of enzymatic phenotypes, Arch. Biochem. Biophys. 682 (2020), 108263.

[6] R. Montioli, G. Janson, A. Paiardini, M. Bertoldi, C.Borri Voltattorni, Heterozygosis in aromatic amino acid decarboxylase deficiency: Evidence for a positive interallelic complementation between R347Q and R358H mutations, IUBMB Life 70 (2018) 215–223.

[7] R. Montioli, R. Battini, A. Paiardini, M. Tolve, M. Bertoldi, C. Carducci, V. Leuzzi, C. Borri Voltattorni, A novel compound heterozygous genotype associated with aromatic amino acid decarboxylase deficiency: Clinical aspects and biochemical studies, Mol. Genet. Metab. 127 (2019) 132–137.

[8] N. Shen, C. Heintz, C. Thiel, J.G. Okun, G.F. Hoffmann, N. Blau, Co-expression of phenylalanine hydroxylase variants and effects of interallelic complementation on in vitro enzyme activity and genotype-phenotype correlation, Mol. Genet. Metab. 117 (2016) 328–335.

[9] R.R. McInnes, V. Shih, S. Chilton, Interallelic complementation in an inborn error of metabolism: genetic heterogeneity in argininosuccinate lyase deficiency, Proc. Natl. Acad. Sci. U. S. A. 81 (1984) 4480–4484.

[10] F.D. Ledley, D.S. Rosenblatt, Mutations in Mut methylmalonic acidemia: clinical and enzymatic correlations, Hum. Mutat. 9 (1997) 1–6.

[11] J. Janata, N. Kogekar, W.A. Fenton, Expression and kinetic characterization of methylmalonyl-CoA mutase from patients with the mut- phenotype: evidence for naturally occurring interallelic complementation, Hum. Mol. Genet. 6 (1997) 1457–1464.

[12] R. Montioli, A. Roncador, E. Oppici, G. Mandrile, D.F. Giachino, B. Cellini, C.Borri Voltattorni, S81L and G170R mutations causing Primary Hyperoxaluria type I in homozygosis and heterozygosis: an example of positive interallelic complementation, Hum. Mol. Genet. 23 (2014) 5998–6007.

[13] T.G. Schmidt, J. Koepke, R. Frank, A. Skerra, Molecular interaction between the strep-tag affinity peptide and its cognate target, streptavidin, J. Mol. Biol. 255 (1996) 753–766.

[14] A.F. Sherald, J.C. Sparrow, T.R. Wright, A spectrophotometric assay for Drosophila dopa decarboxylase, Anal. Biochem. 56 (1973) 300–305.

[15] A. Charteris, R. John, An investigation of the assay of dopamine using trinitrobenzensulphonic acid, Anal. Biochem. 66 (1975) 365–371.

[16] M. Bertoldi, C.Borri Voltattorni, Reaction of dopa decarboxylase with L-aromatic amino acids under aerobic and anaerobic conditions, Biochem. J. 352 Pt 2 (2000) 533–538.

[17] C. Manegold, G.F. Hoffmann, I. Degen, H. Ikonomidou, A. Knust, M.W. Laass, M. Pritsch, E. Wilichowski, F. Hörster, Aromatic L-amino acid decarboxylase deficiency: clinical features, drug therapy and follow-up, J. Inherit. Metab. Dis. 32 (2009) 371–380.

[18] R. Montioli, B. Cellini, C. Borri Voltattorni, Molecular insights into the pathogenicity of variants associated with the aromatic amino acid decarboxylase deficiency, J. Inherit. Metab. Dis. 34 (2011) 1213–1224.

[19] A.I. Denesyuk, K.A. Denessiouk, T. Korpela, M.S. Johnson, Phosphate group binding "cup" of PLP-dependent and non-PLP-dependent enzymes: leitmotif and variations, Biochim. Biophys. Acta 1647 (2003) 234–238.

[20] R. Wolfenden, L. Andersson, P.M. Cullis, C.C. Southgate, Affinities of amino acid side chains for solvent water, Biochemistry 20 (1981) 849–855.

[21] J. Chang, A.M. Lenhoff, S.I. Sandler, Solvation free energy of amino acids and side-chain analogues, J. Phys. Chem. B 111 (2007) 2098–2106.

[22] J. Leandro, C. Nascimento, I.T. de Almeida, P. Leandro, Co-expression of different subunits of human phenylalanine hydroxylase: evidence of negative interallelic complementation, Biochim. Biophys. Acta 1762 (2006) 544–550.

[23] J. Leandro, P. Leandro, T. Flatmark, Heterotetrameric forms of human phenylalanine hydroxylase: co-expression of wild-type and mutant forms in a bicistronic system, Biochim. Biophys. Acta 1812 (2011) 602–612.

[24] C. Heintz, R.G. Cotton, N. Blau, Tetrahydrobiopterin, its mode of action on phenylalanine hydroxylase, and importance of genotypes for pharmacological therapy of phenylketonuria, Hum. Mutat. 34 (2013) 927–936.

[25] R. Montioli, E. Oppici, B. Cellini, A. Roncador, M. Dindo, C.B. Voltattorni, S250F variant associated with aromatic amino acid decarboxylase deficiency: molecular defects and intracellular rescue by pyridoxine, Hum. Mol. Genet. 22 (2013) 1615–1624.

[26] M.M. Verbeek, P.B. Geurtz, M.A. Willemsen, R.A. Wevers, Aromatic L-amino acid decarboxylase enzyme activity in deficient patients and heterozygotes, Mol. Genet. Metab. 90 (2007) 363–369.